








RESEARCH ARTICLE

10.1029/2022JG006997

The Combined Impact of Canopy Stability and Soil NO_x Exchange on Ozone Removal in a Temperate Deciduous Forest

Auke J. Visser¹ , Laurens N. Ganzeveld¹, Angelo Finco² , Maarten C. Krol^{1,3} ,
Riccardo Marzuoli² , and K. Folkert Boersma^{1,4} 

¹Meteorology and Air Quality Section, Wageningen University, Wageningen, The Netherlands, ²Department of Mathematics and Physics, Università Cattolica del Sacro Cuore, Brescia, Italy, ³Institute for Marine and Atmospheric Research Utrecht, Utrecht University, Utrecht, The Netherlands, ⁴Royal Netherlands Meteorological Institute, R&D Satellite Observations, De Bilt, The Netherlands

Special Section:

Advances in scaling and modeling of land-atmosphere interactions

Key Points:

- We use a multi-layer canopy-atmosphere exchange model to interpret ozone flux observations inside and above a North-Italian forest
- Two state-of-science vertical exchange parameterizations do not capture in-canopy stable stratification suppressing ozone deposition
- Soil nitric oxide emissions do not increase ozone deposition due to compensating effects by deposition and transport

Supporting Information:

Supporting Information may be found in the online version of this article.

Correspondence to:

A. J. Visser,
auke.visser@wur.nl

Citation:

Visser, A. J., Ganzeveld, L. N., Finco, A., Krol, M. C., Marzuoli, R., & Boersma, K. F. (2022). The combined impact of canopy stability and soil NO_x exchange on ozone removal in a temperate deciduous forest. *Journal of Geophysical Research: Biogeosciences*, 127, e2022JG006997. <https://doi.org/10.1029/2022JG006997>

Received 11 MAY 2022

Accepted 22 SEP 2022

Author Contributions:

Conceptualization: Auke J. Visser, Laurens N. Ganzeveld, K. Folkert Boersma

Data curation: Angelo Finco, Riccardo Marzuoli

Formal analysis: Auke J. Visser

Funding acquisition: Laurens N. Ganzeveld

© 2022. The Authors.

This is an open access article under the terms of the [Creative Commons Attribution License](https://creativecommons.org/licenses/by/4.0/), which permits use, distribution and reproduction in any medium, provided the original work is properly cited.

Abstract Dry deposition is an important ozone sink that impacts ecosystem carbon and water cycling. Ozone dry deposition in forests is regulated by vertical transport, stomatal uptake, and non-stomatal processes including chemical removal. However, accurate descriptions of these processes in deposition parameterizations are hindered by sparse observational constraints on individual sink terms. Here we quantify the contribution of canopy-atmosphere turbulent exchange and chemical ozone removal by soil-emitted nitric oxide (NO) to ozone deposition in a North-Italian broadleaf deciduous forest. We apply a multi-layer canopy exchange model to interpret campaign observations of nitrogen oxides (NO_x = NO + NO₂) and ozone exchange above and inside the forest canopy. Two state-of-science parameterizations of in-canopy vertical diffusivity, based on above-canopy wind speed or stability, do not reproduce the observed exchange suppressed by canopy-top radiative heating, resulting in overestimated dry deposition velocities of 10%–19% during daytime. Applying observation-derived vertical diffusivities in our simulations largely resolves this overestimation. Soil emissions are an important NO_x source despite the observed high background NO_x levels. Soil NO_x emissions decrease the gradient between canopy and surface layer NO_x mixing ratios, which suppresses simulated NO_x deposition by 80% compared to a sensitivity simulation without soil emissions. However, a sensitivity analysis shows that the enhanced chemical ozone sink by reaction with soil-emitted NO is offset by increased vertical ozone transport from aloft and suppressed dry deposition. Our results highlight the need for targeted observations of non-stomatal ozone removal and turbulence-resolving deposition simulations to improve quantification and model representation of forest ozone deposition.

Plain Language Summary Ozone is a harmful air pollutant that impacts human and ecosystem health. Ozone can be removed by forest ecosystems as a result of air transport into forests followed by plant ozone uptake or chemical removal, but quantifying these individual processes is difficult. We combine model simulations and treetop measurements to study the role of vertical forest-atmosphere air transport and chemical ozone removal inside the forest. We find that our model can only reproduce surface ozone removal if we account for suppressed transport as derived from observations. The soil is a substantial source of nitric oxide (NO) that reacts with ozone. According to our analysis, the presence of a soil NO source does not lead to increased ozone removal because other ozone sinks are reduced. Our results suggest that individual ozone removal processes in forests can best be studied using targeted observations and models that better resolve forest-atmosphere exchange.

1. Introduction

Removal of ozone at the land surface (ozone dry deposition) is an important component of the tropospheric ozone budget, accounting for 15%–20% of the total tropospheric ozone sink (Bates & Jacob, 2020; Hu et al., 2017; Young et al., 2018). Ozone dry deposition occurs when air masses, transported downward by turbulent motions in the atmospheric boundary layer, come in contact with the land surface. Forests are particularly efficient ozone sinks (e.g., Hardacre et al., 2015): removal processes include plant uptake through stomata and various non-stomatal sinks such as external leaf surfaces and soils, and chemical removal in the canopy airspace (Fowler et al., 2009). Upon stomatal uptake, ozone may impact stomatal conductance and photosynthesis, reducing ecosystem carbon assimilation on large spatial scales (Ainsworth et al., 2012). Better quantitative estimates

Methodology: Auke J. Visser, Laurens N. Ganzeveld

Software: Auke J. Visser, Laurens N. Ganzeveld

Supervision: Laurens N. Ganzeveld, K. Folkert Boersma

Visualization: Auke J. Visser

Writing – original draft: Auke J. Visser

Writing – review & editing: Laurens N. Ganzeveld, Angelo Finco, Maarten C. Krol, Riccardo Marzuoli, K. Folkert Boersma

of stomatal and non-stomatal ozone sinks can improve understanding and quantification of the total land surface ozone sink and impacts on ecosystem carbon uptake driven by stomatal ozone uptake.

Stomatal uptake typically accounts for 40%–90% of forest ozone uptake during the growing season (Fowler et al., 2009), but the contribution by individual sink terms is poorly constrained by parameterizations of land-atmosphere exchange in global and regional atmospheric chemistry models (Clifton et al., 2020). Multi-parameterization intercomparisons indicate that these uncertainties lead to a large spread in simulated ozone deposition, attributed to the description of stomatal and various non-stomatal ozone removal processes (Otu-Larbi et al., 2021; Visser et al., 2021; Wu et al., 2018). Likewise, Clifton et al. (2017) found that inter-annual variability in the ozone deposition velocity in a global atmospheric chemistry model was underestimated by a factor two compared to an 11-year ozone flux data set, and attributed this to year-to-year variability in non-stomatal removal. Global model simulations of ozone deposition carry considerable uncertainty (Hardacre et al., 2015; Young et al., 2018), and an effort to quantify inter-model spread of ozone deposition in regional air quality models is currently underway (Galmarini et al., 2021). Altogether, these findings highlight the need for improved process understanding of ozone deposition. In this study, we focus on two of these uncertain processes: in-canopy turbulent exchange and ozone scavenging by soil-emitted nitric oxide (NO). These processes are not explicitly considered in commonly applied “big leaf” representations of dry deposition. Additionally, the scarcity of observational constraints on these processes limit our understanding of the contribution of these processes to forest ozone deposition.

Vertical mixing conditions inside forests can be different compared to those above the canopy, leading to an inversion at the canopy top or inside the canopy, regulated by meteorological conditions and forest structure (Russell et al., 2018). This can lead to a (partial) decoupling between the canopy and the overlying air layers, with implications for canopy-atmosphere gas exchange (e.g., Foken et al., 2012). For example, in-canopy inversions can lead to a missing soil carbon respiration contribution to above-canopy measurements of net ecosystem exchange of CO₂ (Jocher et al., 2018). For ozone, several studies suggest a dependence of ozone deposition on in-canopy turbulent mixing based on correlations between the deposition velocity and the friction velocity (e.g., El-Madany et al., 2017; Fares et al., 2014; Neiryck et al., 2012). Van Pul and Jacobs (1994) derived such a parameterization from measurements over maize crop, but its applicability to other land use categories remains uncertain. Multi-layer canopy-atmosphere exchange models typically simulate vertically resolved in-canopy and canopy-surface layer turbulent exchange based on K-theory (e.g., Ashworth et al., 2015; Ganzeveld, Lelieveld, Dentener, Krol, & Roelofs, 2002). This formulation has strong limitations when applied in forest canopies, where the dependency between time-averaged gradients and fluxes can become invalid due to the occurrence of coherent turbulent structures, stable mixing conditions or more than one emission or deposition source (Bannister et al., 2022; Finnigan, 2000). Inferring in-canopy mixing conditions from observations requires vertical profile measurements of temperature and the sensible heat flux (e.g., Brown et al., 2020), which are not typically available at flux measurement sites. Therefore, the simplified representation of canopy-atmosphere exchange in current models and the sparse observational constraints limit our understanding of the role of turbulent mixing in canopy ozone removal.

Chemical ozone removal in plant canopies is another poorly constrained element of the ozone deposition sink. The canopy has a distinctly different photo-chemical regime compared to the surface layer affected by radiation extinction, emissions of soil NO and biogenic volatile organic compounds (BVOCs), as well as deposition processes. In big leaf parameterizations, it is common practice to emit soil NO directly into the surface layer after application of a canopy reduction factor (CRF), thereby only implicitly accounting for in-canopy NO_x removal. Therefore, these parameterizations do not account for the different photo-chemical regime inside the canopy. Observation-based studies indicate a widely varying contribution of chemical ozone removal by soil NO and BVOCs, that largely depends on site-specific characteristics such as soil and plant type, temperature, soil moisture and vapor pressure deficit (Fares et al., 2012; Finco et al., 2018; Rannik et al., 2012; Vermeuel et al., 2021). In Europe, anthropogenic NO_x and VOC sources are decreasing (Kuenen et al., 2022). As a result, agricultural and forest soils are becoming an increasingly important component of the European NO_x emission budget (Skiba et al., 2021), that contribute to ozone formation particularly during NO_x-limited ozone formation conditions (Visser et al., 2019). Soil-emitted NO also act as an ozone sink inside forest canopies depending on the emission strength and canopy radiation extinction, leading to a locally NO_x-saturated ozone production regime. Commonly used parameterizations of soil-biogenic NO_x emissions in chemical transport models assume that forest soil NO

emissions are relatively small compared to anthropogenic emissions, but are an important source of NO_x in pristine environments (Yienger & Levy, 1995). For example, Rummel et al. (2007) found that soil NO-ozone chemistry is a substantial component of the nighttime ozone sink in a tropical forest. In more polluted environments, nitrogen deposition accumulated over multiple years may substantially increase forest soil NO_x emissions (Pilegaard et al., 2006). Under such circumstances, soil NO-ozone chemistry may explain a considerable part of total ozone deposition even during daytime (Dorsey et al., 2004; Duyzer et al., 2004).

In this study, we aim to investigate the combined impact of canopy stability and soil NO emissions in the canopy airspace on ozone fluxes. We interpret field campaign observations of vertical gradients in ozone uptake in the North-Italian Bosco Fontana forest, experiencing substantial NO_x and ozone air pollution (Finco et al., 2018). This analysis of field observations is supported by observation-driven simulations with the Multi-Layer Canopy-CHEMistry Exchange Model (MLC-CHEM) (Ganzeveld, Lelieveld, Dentener, Krol, & Roelofs, 2002; Visser et al., 2021). Specifically, we address the following research questions for a temperate mid-latitude forest:

1. How does the representation of vertical exchange in a multi-layer canopy model affect simulated canopy ozone uptake?
2. What is the contribution of soil and canopy-top NO_x fluxes to observed NO_x mixing ratios inside and above the canopy?
3. What is the contribution of NO_x -ozone chemistry to in-canopy ozone removal under different model representations of vertical exchange?

2. Data and Methods

2.1. Observations

We use atmosphere-biosphere exchange measurements obtained during an observational campaign in June 2012–July 2012 at the Bosco Fontana deciduous forest in northern Italy (45.20°N, 10.74°E) (Finco et al., 2018). This campaign took place within the European project “Effects of Climate Change on Air Pollution Impacts and Response Strategies for European Ecosystems”. This forested site is situated in the Po Valley, in a 235 ha natural reserve composed primarily of *Carpinus betulus L.* and *Quercus robur L.*, and the average canopy height is 26 m above ground level (Gerosa et al., 2017).

The Po Valley is characterized by warm summers and high concentrations of ozone and nitrogen oxides. Under such conditions, hydrological interactions leading to droughts reduce the stomatal ozone sink (Lin et al., 2020). Whether this results in an overall decrease in dry deposition depends on the behavior of non-stomatal deposition during droughts, and observational evidence suggests that non-stomatal deposition may increase under these conditions (Agyei et al., 2020; Wong et al., 2022). The summer of 2012 was characterized by slightly drier meteorological conditions ($\pm 1\sigma$) compared to the long-year average around Bosco Fontana, while the area south of the Po Valley experienced dry conditions (Figure 1b, more details can be found in Text S1 in Supporting Information S1).

We compared the drought signal to a data set of stomatal ozone fluxes derived from flux tower measurements (Ducker et al., 2018, see Text S1 in Supporting Information S1 for more details). The stomatal ozone flux does not exceed $3 \text{ nmol m}^{-2} \text{ s}^{-1}$ and is up to 50% lower compared to the multi-year summer average value (Figure 1). This is likely caused by stomatal closure as a result of drought conditions. In the (pre-)alpine regions north of Bosco Fontana, conditions are slightly wetter than average, and stomatal ozone fluxes are higher ($>4 \text{ nmol m}^{-2} \text{ s}^{-1}$) compared to the south, with no clear indication of a regional anomaly (Figure 1b). We therefore deem these observations representative for typical summer conditions in North Italy.

We here focus on the period of 24 June 2012–11 July 2012, when temperature, wind speed, humidity, ozone, and NO_x concentrations as well as fluxes of sensible heat and ozone were measured along a vertical profile inside and above the canopy at the Bosco Fontana site. Ozone fluxes were measured with the eddy covariance technique. The fast ozone sensors applied during this campaign were the ROFI (CEH, UK) at 32 m and the FROM (NOAA, USA) at 24 m. Specifically, measurements were performed at two heights above the canopy top (41 and 32 m), at the interface layer between the canopy and the surface layer (24 m) and at two heights inside the canopy (8 and 16 m). More details on the observational setup and flux data processing can be found in Finco et al. (2018).

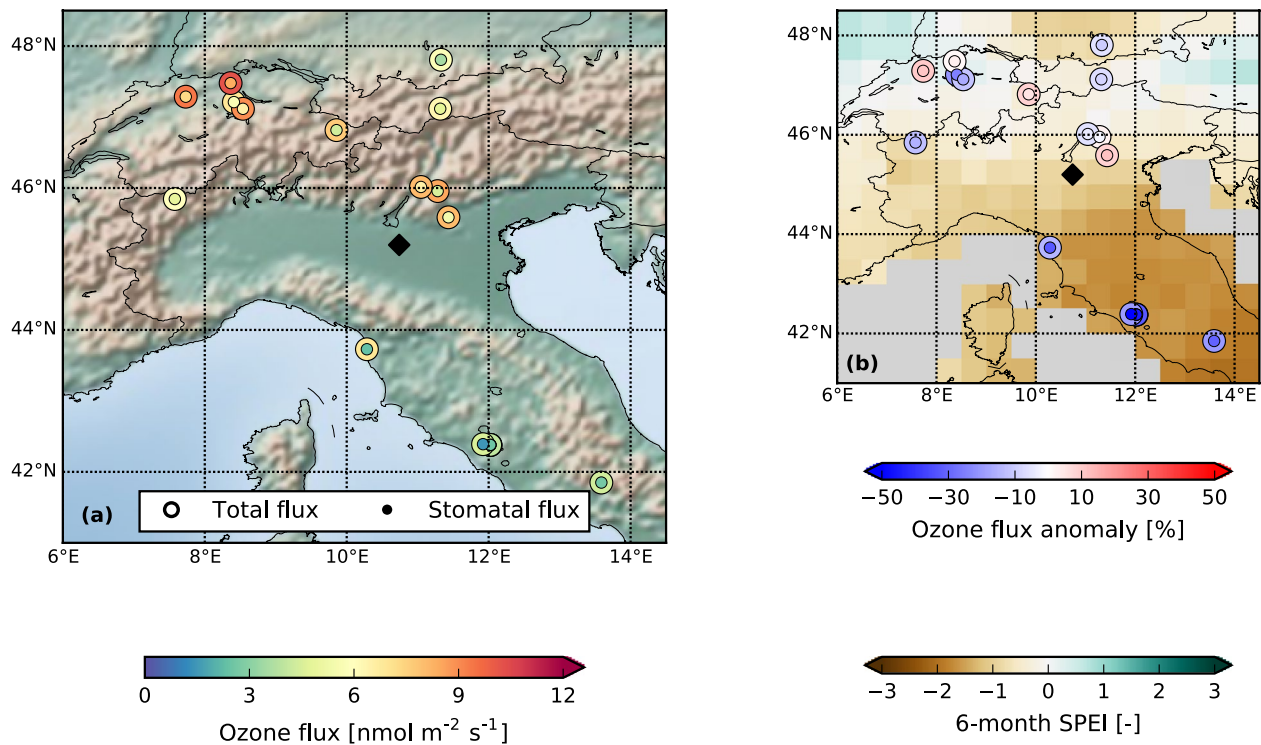


Figure 1. Summer 2012 ozone fluxes around northern Italy in a spatio-temporal context. (a) June–August average daytime total (outer circles) and stomatal (inner circles) ozone fluxes derived from observations at FLUXNET locations (data from Duckert et al., 2018). (b) July–August normalized 6-month SPEI anomaly (gridded data, derived from <https://spei.csic.es/index.html>, last access 24 March 2022), where negative (positive) values indicate drier (wetter) than average conditions, and the total and stomatal ozone flux relative anomaly compared to the observational record at the FLUXNET location. Bosco Fontana is indicated with a black diamond in both figures. See Text S1 in Supporting Information S1 for details on the SPEI and SynFlux data analysis.

2.2. The Multi-Layer Canopy-Chemistry Exchange Model (MLC-CHEM)

We perform biosphere-atmosphere trace gas exchange simulations using the MLC-CHEM. This model simulates atmosphere-biosphere exchange fluxes and vertical profiles of trace gases, and includes a representation of BVOCs emissions (Guenther et al., 2012) and soil NO emissions (Yienger & Levy, 1995), in-canopy vertical mixing, a complex chemistry scheme (CBM-IV) and dry deposition of atmospheric compounds (Ganzeveld & Lelieveld, 1995; Ganzeveld et al., 1998). Stomatal conductance is calculated using the assimilation-stomatal conductance model $A-g_s$ (Ronda et al., 2001), with parameter settings based on the observation-derived values from Visser et al. (2021). The $A-g_s$ parameters used in this study are shown in Table S1 in Supporting Information S1. With these settings, MLC-CHEM reproduces observation-derived stomatal conductance (calculated following Monteith, 1965), and the canopy-atmosphere CO₂ exchange flux well (Figure S2 in Supporting Information S1).

In this study, we force MLC-CHEM with canopy-top observations of net shortwave radiation, temperature, relative humidity, wind speed, friction velocity and surface-layer NO, NO₂, and ozone mixing ratios. MLC-CHEM simulates in-canopy mixing ratios and fluxes of these species as affected by the aforementioned sources and sinks inside the canopy. We further highlight MLC-CHEM's representation of vertical exchange and soil NO emissions in the sections below.

In the set-up of MLC-CHEM in this study, the model consists of three layers: one bulk atmospheric surface layer, and a crown and understory layer that together represent the forest canopy. This set-up of the model has also been coupled to large-scale atmospheric chemistry models (Ganzeveld et al., 2010; Ganzeveld, Lelieveld, Dentener, Krol, Bouwman, & Roelofs, 2002). In-canopy radiation is expected to display large gradients between canopy-top and soil, and therefore processes affected by radiation (photolysis and biogenic emissions) are calculated in more vertical detail using four layers. Although MLC-CHEM can in principle be applied at a higher vertical resolution

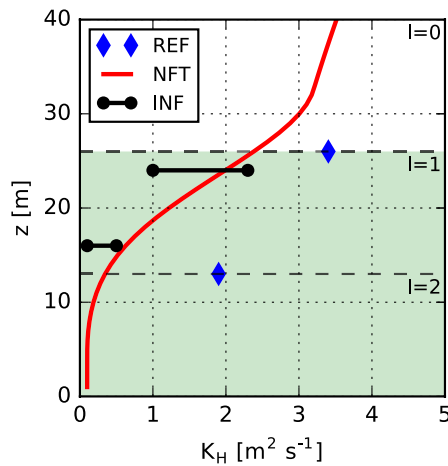


Figure 2. Schematic representation of typical afternoon vertical profiles of vertical diffusivity (K_H) in the Bosco Fontana forest (indicated by the green shaded area) in an unstable mixing regime. The reference Multi-Layer Canopy-CHEMistry Exchange Model (MLC-CHEM) vertical mixing parameterization (REF) is shown in blue diamonds and the near-field theory parameterization (near-field theory) is indicated by the red line. These profiles are calculated using $u_* = 0.5 \text{ m s}^{-1}$, $u = 2 \text{ m s}^{-1}$, $K_H(z_{ref}) = 4 \text{ m}^2 \text{ s}^{-1}$ (at a reference height of 50 m), $r_a = 20 \text{ s m}^{-1}$. Solid black lines and points show the mid-day (12–15 hr LT) range of observation-inferred K_H values at two different heights. Dashed black lines indicate the interface between model layers in MLC-CHEM. The index l (varying from 0 to 2) refers to the model layers in Equation 1.

(i.e., with more than two canopy layers), we can only derive vertical transport from observations at two heights inside the canopy (see Section 2.3.3 and Figure 2). This motivates our use of the two-layer version in this study.

2.3. Vertical Mixing in MLC-CHEM

We here test two methods of simulating turbulent exchange between atmosphere and the canopy, and compare these to exchange simulations with observation-derived vertical exchange. These representations will be introduced in this section, and are schematically visualized in Figure 2.

2.3.1. Reference Parameterization of Turbulent Exchange (REF)

MLC-CHEM's default parameterization of turbulent exchange between canopy and the surface layer derives the surface-layer to upper canopy eddy diffusivity (denoted as $K_{H,sl}$) by integrating the aerodynamic conductance over the difference in reference height between the surface layer and the upper canopy layer, following Monin-Obukhov Similarity Theory. The in-canopy eddy diffusivity ($K_{H,cl}$), used to calculate turbulent exchange between the crown layer and the understory layer, is then derived by scaling $K_{H,sl}$ with the in-canopy wind speed profile (Ganzeveld, Lelieveld, Dentener, Krol, & Roelofs, 2002):

$$K_{H,cl} = K_{H,sl} \frac{0.5(u(l) + u(l-1))}{0.5(u(1) + u(0))} \quad (1)$$

where $u(l)$ is the horizontal wind speed at layer l (index values 0, 1, and 2 represent the bulk surface layer, the upper canopy layer, and the lower canopy layer, respectively, as shown in Figure 2). The simulated in-canopy

wind speed decreases exponentially as a function of canopy height and canopy-specific attenuation coefficients (Cionco, 1978). Figure 2 displays typical mid-day values of the vertical diffusivity as derived from MLC-CHEM. During typical summer afternoon conditions characterized by efficient vertical mixing above the canopy, in-canopy K_H is typically a factor ± 7 lower than canopy-top K_H due to the scaling by the in-canopy wind speed.

2.3.2. Near-Field Theory (NFT)

We additionally apply a parameterization based on near-field theory (Raupach, 1989), which has resulted in improved surface ozone simulations with an online chemistry transport model (CTM) over forested regions in the United States (Makar et al., 2017). This formulation accounts for a decrease in the turbulent mixing intensity inside and above the forest with respect to the reference height of the lowermost model layer, resulting from obstruction of air flow due to the presence of trees. In this parameterization, $K_{H,sl}$ in the lowermost model layer of the CTM is scaled down toward the land surface as a function of canopy height, friction velocity, and the Obukhov length. Figure 2 shows how the NFT vertical diffusivity decreases toward the surface in this formulation as a result of canopy influences on turbulence intensity. K_H at the canopy-top is particularly smaller in NFT compared to the reference parameterization in MLC-CHEM (REF). In-canopy K_H is relatively similar in both formulations.

2.3.3. Observation-Inferred Turbulent Exchange Derivation (INF)

Third, we derive the turbulent exchange coefficient from observations following K -theory. This theory relates the observed sensible heat flux to the observed vertical potential temperature gradient via the vertical diffusivity coefficient K_H :

$$H(z) = -K_H(z) \frac{\delta\theta(z)}{\delta z} \quad (2)$$

where $H(z)$ is the observed sensible heat flux at height z and $\frac{\delta\theta(z)}{\delta z}$ is the vertical potential temperature gradient at height z , inferred from temperature measurements above and below z . This slope is derived by fitting potential temperature to the curve $\theta = a + b \times \ln(z) + c \times \ln(z)^2$ (Brown et al., 2020; Mölder et al., 1999). We here apply the vertical diffusivity derived from observed vertical profiles of temperature and the sensible heat flux in our

simulations of ozone and NO_x canopy-atmosphere exchange, assuming that exchange coefficients of these gases resemble the exchange coefficient of heat. We will revisit this assumption in the discussion, by performing a comparison with exchange coefficients derived from vertical gradients of ozone concentrations and fluxes.

We calculate $K_H(z)$ at two different heights within the canopy. K_H is calculated at the canopy-surface layer interface from 30-min averages of sensible heat fluxes measured at 24 m and temperature gradients between 16 and 32 m. In-canopy K_H is derived from 30-min averages of sensible heat fluxes measured at 16 m and temperature gradients between 8 and 24 m. Figure 2 displays the typical mid-day K_H range as derived from observations. Note that we apply $K_{H,24m}$ for simulating exchange at the canopy-top, so these values are shown at $z = 26\text{m}$. $K_{H,16m}$ is used for simulating vertical exchange between the crown and understory layers ($z = 13\text{m}$). The observation-inferred K_H is lower than REF and NFT at the canopy-top, and the mid-canopy values of REF and NFT approximately coincide with the upper value of the observation-inferred K_H range.

2.4. Soil NO_x Exchange

We perform an initial evaluation of MLC-CHEM-simulated NO_x mixing ratios in the understory to understand the role of soil NO_x exchange on observed NO_x mixing ratios at Bosco Fontana. A simulation with the default deciduous forest soil NO emission factor from (Yienger & Levy, 1995) results in an emission strength of 0.2–0.6 $\text{ng N m}^{-2} \text{s}^{-1}$ (Figure S3a in Supporting Information S1). This is substantially lower than the site-derived emission flux of 20.8 $\text{ng N m}^{-2} \text{s}^{-1}$, based on enclosure chamber measurements directly above the Bosco Fontana forest floor (Finco et al., 2018). As a result, MLC-CHEM-simulated understory NO_x mixing ratios using the default deciduous forest emission factor are underestimated by 2.1 ppb (27%) on average (Figure S3c in Supporting Information S1).

However, imposing the observation-derived soil NO emission flux in MLC-CHEM leads to an overestimation of understory NO_x mixing ratios by 3.1 ppb (37%) compared to observations, reflecting NO_x accumulation (Figure S3c in Supporting Information S1). These over-estimations in simulated lower-canopy $[\text{NO}_x]$ result partly from an underestimated NO_2 deposition sink in MLC-CHEM (1–6 $\text{ng N m}^{-2} \text{s}^{-1}$) that is more than a factor two smaller compared to the observation-derived soil NO_2 deposition flux of $\pm 14 \text{ng N m}^{-2} \text{s}^{-1}$ (Finco et al., 2018). A sensitivity test assuming a strongly enhanced soil uptake efficiency of NO_2 , by reducing MLC-CHEM's NO_2 soil uptake resistance from 600 to 100 s m^{-1} , does not strongly increase simulated soil NO_2 deposition. Additionally, there are strong observed vertical gradients in NO_x mixing ratios near the soil, reflecting strongly stable conditions and NO_x loss due to chemical removal and soil deposition, which are not represented in MLC-CHEM's understory layer with a thickness of 13 m. This indicates that a substantial part of the soil-emitted NO_x does not escape the air layer directly above the soil.

In order to infer the contribution of soil NO_x exchange to observed NO_x mixing ratios at the reference height of MLC-CHEM's understory layer ($z = 6.5 \text{m}$), we study the sensitivity of simulated understory NO_x to the soil NO emission flux. By comparison with observed NO_x mixing ratios in the understory, we find that application of a reduced soil NO emission strength of 8 $\text{ng N m}^{-2} \text{s}^{-1}$ minimizes the mismatch between simulated and observed understory NO_x (Figure S3c in Supporting Information S1), and we therefore choose this value to represent the effect of soil NO_x exchange on canopy ozone uptake for our simulations. Note that we do not consider a leaf-level NO_2 compensation point. Previous studies have indicated a maximum leaf-level NO_2 compensation point of 1–3 ppb (Raivonen et al., 2009; Teklemariam & Sparks, 2006, and references therein), while the minimum observed ambient NO_2 levels at Bosco Fontana are ± 3 ppb. Additionally, recent observational evidence suggests that this value does not differ significantly from zero (Delaria et al., 2018; Wang et al., 2020).

2.5. Setup of the Numerical Experiments

In order to answer our research questions, we modify the representation of in- and above-canopy vertical mixing, as well as soil NO_x exchange, in MLC-CHEM. The reference simulation (Experiment 1) applies the model's reference vertical diffusivity formulation (REF), a default temperate forest soil NO emission factor (Yienger & Levy, 1995) and the standard soil NO_2 uptake resistance (Ganzeveld & Lelieveld, 1995). In Experiments 2–4, we modify MLC-CHEM's vertical exchange formulation as explained in Section 2.3. We use the effective soil NO emission flux that best represents soil effects on lower-canopy NO_x mixing ratios and the default NO_2 uptake

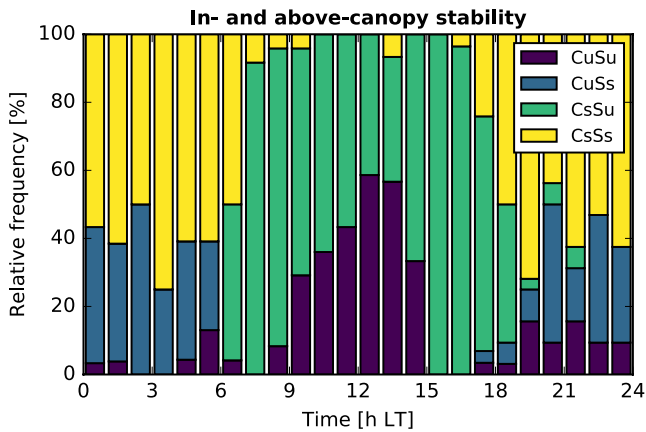


Figure 3. Occurrence of in- and above-canopy stability classes during the observational time period (24 June 2012–12 July 2012). Data were separated into four stability classes, based on stability parameter $\frac{z}{L}$ as unstable (lowercase u , $\frac{z}{L} < 0$) or stable (lowercase s , $\frac{z}{L} > 0$), as well as height of the observations, being representative of the surface layer (uppercase S , derived from observations at 32 m) or inside the canopy (uppercase C , derived from observations at 16 m).

resistance (Section 2.4). In Experiments 5–7, we deactivate soil NO emissions and soil NO_2 deposition to quantify the effect of soil NO_x exchange on in-canopy NO_x mixing ratios and ozone deposition.

3. Results

3.1. Vertical Exchange

We start our analysis by examining temporal variability in the observation-derived vertical diffusivity (K_H) and its relation to in- and above-canopy stability. Figure 3 displays the stability regimes in the surface layer and the canopy. Stably stratified conditions occur frequently inside the canopy even during daytime (Figure 3), resulting from radiative heating of the canopy-top and a closed canopy structure that prevent the warm above-canopy air from entering the canopy airspace (Finco et al., 2018). Observation-inferred K_H at the interface between the canopy and the overlying air layer ($z = 24$ m) peaks at $2.4 \text{ m}^2 \text{ s}^{-1}$ at 15:30 LT (Figure 4b), coinciding with prevailing unstable mixing conditions above the canopy (Figure 3). The campaign-average diurnal cycle of the observation-derived K_H inside the canopy ($z = 13$ m) is characterized by lower values throughout the day (up to $0.5 \text{ m}^2 \text{ s}^{-1}$, Figure 4d), reflecting the decrease in vertical mixing inside the forest canopy (Figure 2). Mid-canopy K_H derived from observations peaks at 11:30–12:00 LT (Figure 4d), coinciding with predominantly unstable conditions inside and above the canopy.

Contrary to the observations, simulated K_H according to the REF approach in MLC-CHEM follows a symmetric diurnal profile peaking at 13:00 LT (Figure 4b), which is substantially larger compared to the observation-inferred K_H during daytime. The K_H overestimation results from the simplified K_H derivation in this model setup (see Section 2.3.1). As a result, REF-simulated vertical exchange at the canopy-top is overestimated compared to observation-inferred K_H (Figure 4b). The REF-simulated in-canopy K_H shows substantial day-to-day variation due to its dependence on above-canopy wind speed (Section 2.3.1), and strongly overestimates K_H inside the

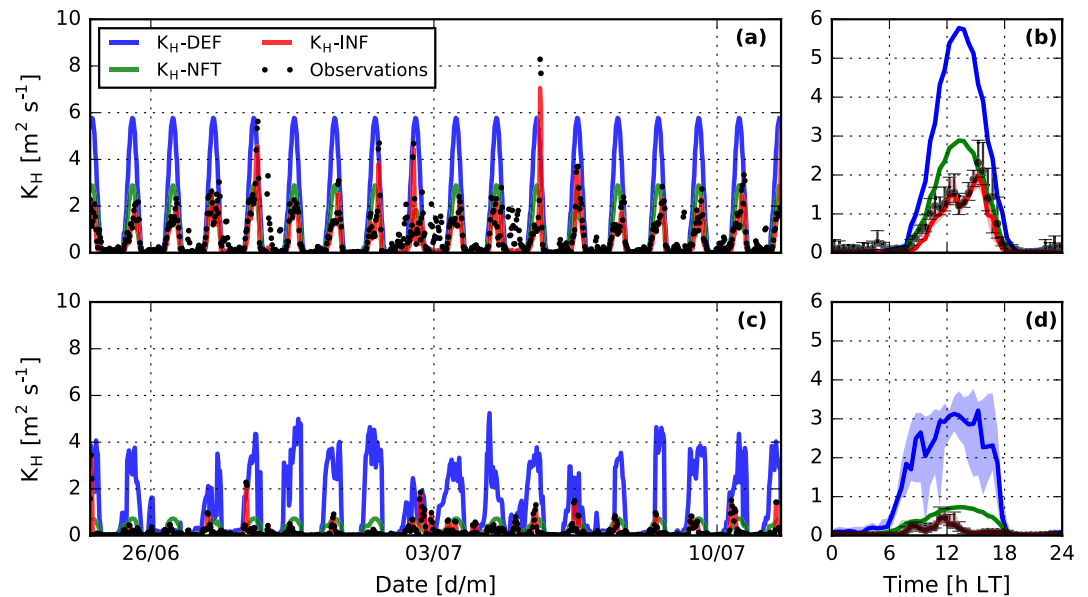


Figure 4. Time series (a and c) and campaign-average diurnal cycle (b and d) of vertical diffusivity at the canopy-surface layer interface (a and b) and 13 m, halfway the canopy (c and d), as derived from observations (black dots), and as calculated from three Multi-Layer Canopy-Chemistry Exchange Model simulations (solid lines, see Section 2.3) Black lines and shaded areas indicate the inter-quartile range.

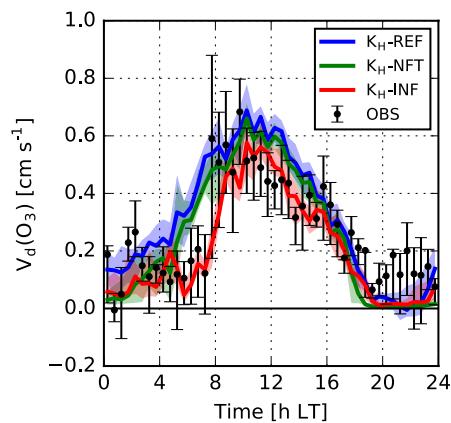


Figure 5. Campaign-median diurnal cycle of the ozone dry deposition velocity derived from observations (black points and whiskers), and simulated by Multi-Layer Canopy-Chemistry Exchange Model (MLC-CHEM) with three different K_H derivations: MLC-CHEM's reference vertical diffusivity description (REF), near-field theory, and observation-inferred K_H (INF). The observation-inferred deposition velocity ($V_d(O_3) = \frac{F_{O_3}}{[O_3]}$) at the canopy-atmosphere interface (26 m) is derived by linear interpolation between observations at 24 and 32 m.

canopy leading to well-mixed conditions inside the canopy during daytime in this simulation. As a result, vertical exchange is strongly overestimated in the REF vertical exchange representation in MLC-CHEM compared to observation-inferred vertical mixing during the observational campaign.

Canopy-top K_H from a simulation based on NFT follows a similar diurnal cycle compared to REF, since NFT is derived from scaling down the REF-simulated vertical diffusivity to include effects of the roughness sublayer (see Section 2.3.2). The NFT-simulated K_H above the canopy is up to $3 \text{ m}^2 \text{ s}^{-1}$ lower compared to the REF simulation during mid-day, and in closer agreement with observation-inferred K_H values. Inside the canopy, the NFT-simulated K_H is also substantially lower compared to the REF K_H , and in closer agreement with observation-inferred values. However, NFT does also not reproduce the observed low afternoon K_H values indicative of stably stratified conditions inside the canopy. In the next section, we will evaluate the effects of these different representations of vertical diffusivity on the simulated ozone and NO_x profiles.

3.2. Effects of Turbulent Mixing on Canopy Ozone Uptake

We analyze the effect of vertical mixing on ozone deposition via the simulated deposition velocity. In MLC-CHEM, vertical mixing affects the canopy-atmosphere transport of ozone and thus the ozone flux. $V_d O_3$ is diagnostically calculated from the ozone flux at the canopy-atmosphere interface

and canopy-top ozone mixing ratios simulated by MLC-CHEM. Figure 5 displays the campaign-median ozone dry deposition velocity ($V_d(O_3)$) diurnal cycle from observations and three MLC-CHEM simulations with different representations of vertical exchange. Observed $V_d(O_3)$ is characterized by nighttime values of $0.0\text{--}0.2 \text{ cm s}^{-1}$, followed by a sudden increase in the morning ($\pm 8 \text{ hr LT}$) to its peak value of 0.7 cm s^{-1} , and a subsequent decrease throughout the day. Notably, the REF and NFT simulations strongly overestimate $V_d(O_3)$ at $5\text{--}8 \text{ hr LT}$, while a simulation with the observation-derived representation of vertical exchange (INF) agrees better with observations during this time period. This coincides with overestimated K_H values in REF and NFT, particularly at mid-canopy, during the early morning (Figure 4d). Neither simulation reproduces the daytime peak value occurring at 8 hr LT , which reflects a sudden change from stable to unstable stratification in the upper canopy. The spread in observed $V_d(O_3)$ at this time is high, indicating that the timing of the change to unstable conditions varies from day-to-day, or a possible role of intermittent exchange. The REF and NFT simulations overestimate daytime $V_d(O_3)$ ($9\text{--}16 \text{ hr LT}$) by 19% and 10%, respectively. INF reproduces daytime $V_d(O_3)$ within 5% of the observations due to accounting for a (partial) decoupling between the canopy and the surface layer.

Despite distinct differences in the simulated diurnal cycle, effects of vertical exchange on MLC-CHEM's performance (shown in Table 2) are small. The similar model performance metrics reflect the compensating effects of model overestimations and underestimations during different stages in the diurnal cycle, as discussed above. The effect of constraining the simulations with observation-derived vertical exchange most strongly reduces overestimations in the simulated ozone flux, as INF reduces the model overestimations from 13% to 16% to 8% (Table 2). When analyzing skill scores for $9\text{--}15 \text{ hr LT}$, when unstable conditions inside and above the canopy are more prevalent, the MBE is markedly lower in the INF simulation ($0.7 \text{ nmol m}^{-2} \text{ s}^{-1}$) compared to the REF and NFT simulations (4.3 and $3.2 \text{ nmol m}^{-2} \text{ s}^{-1}$, respectively). Hence, vertical exchange only minimally affects canopy ozone uptake averaged over the entire day, but the effects are substantial during time periods characterized by (partial) decoupling between canopy and the overlying atmospheric layers.

3.3. Effects of Soil NO_x Exchange on the Canopy NO_x Budget

Biosphere-atmosphere exchange of NO_x can be bi-directional (i.e., emission or deposition), depending on the difference between above- and below-canopy NO_x mixing ratios. Generally, the canopy-atmosphere NO_x flux is downward in (forested) regions with high background NO_x mixing ratios, regardless of the soil NO source strength (Ganzeveld, Lelieveld, Dentener, Krol, Bouwman, & Roelofs, 2002). Elevated NO_x mixing ratios observed at

Table 1
Configuration of Multi-Layer Canopy-CHEMistry Exchange Model Simulations

Experiment	K_H method	$E_{NO_x,soil}$ (ng N m ⁻² s ⁻¹)	$r_{soil}(NO_2)$ (s m ⁻¹)
1	REF	0.2–0.6 ^a	600
2	REF	8	600
3	NFT	8	600
4	INF	8	600
5	REF	0	10 ⁵
6	NFT	0	10 ⁵
7	INF	0	10 ⁵

^aDiurnal range, peaking in the afternoon.

Bosco Fontana (up to 16 ppb in the morning and 4 ppb in the afternoon) therefore suggest that NO_x deposition to the forest canopy is expected to prevail at this site. The observed exchange of NO_x at the soil interface is bi-directional (NO emissions, NO₂ deposition), resulting in a substantial net upward NO_x flux (Finco et al., 2018, see also Section 2.4). We infer the contribution of soil NO_x exchange to in-canopy NO_x mixing ratios by comparing an MLC-CHEM simulation with observation-inferred vertical exchange (INF) to an experiment with deactivated soil NO_x exchange (Experiments 4 and 7 in Table 1). Figure 6 displays observed and MLC-CHEM-simulated upper- and lower-canopy NO_x mixing ratios. As expected, the effect of soil NO_x exchange is largest in the understory, with simulated enhancements in NO_x mixing ratios of 0.6 ppb during daytime to 7.5 ppb at night due to soil NO_x exchange (Figure 6b). Additionally, the simulation without soil NO_x exchange does not lead to nighttime NO_x accumulation in the canopy, and an underestimation of [NO_x] by >5 ppb during nighttime. Our sensitivity simulation suggests that the soil contributes on average 45% to observed

mixing ratios in the understory. The net upward soil NO_x flux additionally affects the simulated diurnal course of lower-canopy NO_x mixing ratios, as the observed evening increase rate in NO_x mixing ratios is absent in the simulation without soil NO_x exchange.

Soil NO_x has a smaller effect on NO_x mixing ratios in the upper canopy layer compared to the understory. NO_x mixing ratios are lower by 0.1 ppb (daytime) up to 3.2 ppb (nighttime) in the simulation without soil NO_x exchange (Figure 6a), and we infer that the soil contributes on average 21% to NO_x mixing ratios in this layer. The soil contribution is lowest during mid-day, when vertical exchange between the upper canopy and the overlying air layer is intense while mixing between the two canopy layers is suppressed (Figures 4b and 4d). Note here that the NO_x concentrations in MLC-CHEM's surface layer are nudged to observations at 32 m. The similarity in the shape of the simulated diurnal cycles suggests that diurnal variation in upper-canopy NO_x mixing ratios is largely driven by the canopy-top NO_x flux. The two simulations diverge after 16 hr LT, when the upper canopy becomes stably stratified, which indicates a substantial contribution of the soil to upper-canopy NO_x levels even at this site with a large NO_x source from advection.

Canopy-atmosphere NO_x exchange is strongly affected by soil NO_x exchange. Figure 7 displays campaign-median diurnal cycles of simulated canopy-top NO_x fluxes with and without considering the contribution by soil NO emissions. The simulated daytime upward canopy-top NO flux is higher by up to 3 ng N m⁻² s⁻¹ due to soil NO_x exchange (Figure 7a). In both simulations, the canopy remains a net sink of NO₂ due to the high background levels observed at this site. However, canopy uptake of NO₂ is reduced due to the effect of soil NO_x emissions (Figure 7b), and even changes in sign at night, as mixing of soil-emitted NO_x into the canopy layers reduces the gradient between canopy and the overlying air layer. As a result of the changing vertical gradient in NO_x mixing ratios between the canopy layers and the surface layer, considering soil NO_x exchange in MLC-CHEM reduces the canopy-top NO_x fluxes by on average 4.5 ng N m⁻² s⁻¹ (–79.8%). This analysis highlights the importance of accounting for soil NO_x exchange for accurately simulating NO_x deposition in larger-scale models for relatively polluted regions.

Table 2
Model Performance Statistics of the Simulated Ozone Flux in Three Multi-Layer Canopy-CHEMistry Exchange Model Simulations With Different Representations of Vertical Exchange

	MBE	RMSE	r^2 (–)	s (–), i	d (–)	$f > 2x$ (–)	$f < 2x$ (–)
REF	1.61	5.5	0.45	0.69, 3.73	0.80	0.16	0.16
NFT	0.75	5.1	0.47	0.70, 2.86	0.82	0.13	0.22
INF	–0.18	4.9	0.45	0.60, 2.63	0.81	0.08	0.23

Note. The table includes several common statistical model performance indicators (MBE, RMSE, r^2 , slope, and intercept of the linear regression fit through simulations and observations (s , i), as well as the index of agreement d (Willmott, 1982), and the fraction of simulated data points overestimated and underestimated by a factor larger than 2 ($f > 2x$ and $f < 2x$), respectively). The unit is nmol m⁻² s⁻¹, unless indicated otherwise.

3.4. Canopy Reduction of NO_x

The simulated canopy-top NO flux is generally smaller than the soil NO flux at Bosco Fontana (Figure 7), which reflects in-canopy NO_x loss. Many large-scale models do not explicitly represent canopy processes, and account for this decrease in the effective contribution by soil NO emissions to atmospheric NO_x mixing ratios by applying a CRF to account for in-canopy removal of the emitted NO_x by NO₂ deposition (Yienger & Levy, 1995). When above-canopy NO_x mixing ratios are smaller compared to the in-canopy NO_x mixing ratio, this CRF has a value between 0 and 1 (Yienger & Levy, 1995),

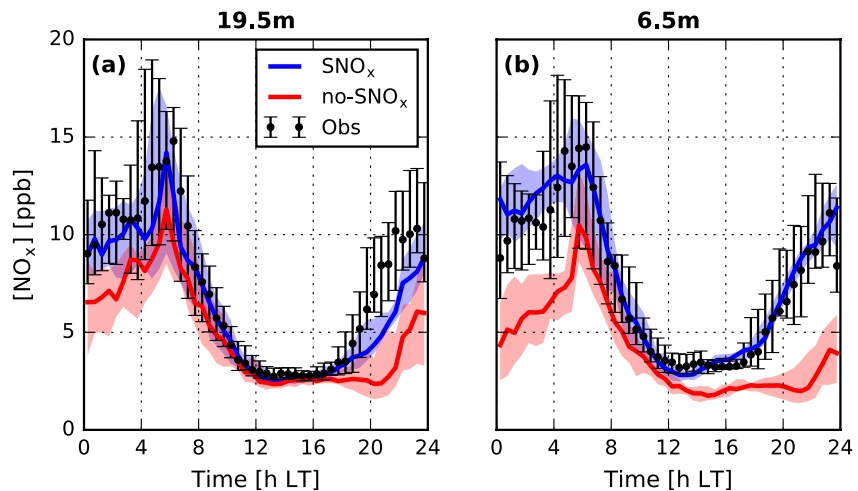


Figure 6. Campaign-median diurnal cycle of NO_x mixing ratios the reference heights of the two canopy layers, as simulated by Multi-Layer Canopy-CHEMistry Exchange Model (with observation-inferred vertical mixing) with (SNO_x , blue line) and without (no- SNO_x , red line) soil NO_x exchange. Observations at 19.5 m are derived by vertical interpolation of measurements at 8 and 24 m, while observations at 5 m are directly compared to model output at 6.5 m. Points and solid lines display the mean, and whiskers and shaded area display the inter-quartile range.

for example, ± 0.75 for midlatitude deciduous forest (Vinken et al., 2014). However, for high- NO_x regions such as northern Italy, an alternative definition of the CRF is more appropriate.

This alternative CRF is derived as the ratio between above-canopy and above-soil NO_x fluxes (Ganzeveld, Lelieveld, Dentener, Krol, Bouwman, & Roelofs, 2002), and reflects the role of in-canopy NO_2 deposition, chemical cycling, and the bi-directionality of canopy-atmosphere NO_x exchange. We derive a CRF of -0.24 (diurnal average), which indicates that the soil NO_x exchange flux is approximately four times higher than the simulated downward canopy-top NO_x flux. This negative estimate reflects that Bosco Fontana is a sink of NO_x , although much closer to zero compared to the CRFs of -10 to -1 found by Ganzeveld, Lelieveld, Dentener, Krol, Bouwman, and Roelofs (2002) over high- NO_x regions in the northern midlatitudes. This relatively small CRF inferred from our canopy-exchange simulations can largely be explained by the large soil NO emission flux at Bosco Fontana: Ganzeveld, Lelieveld, Dentener, Krol, Bouwman, and Roelofs (2002) used emission factors from Yienger and Levy (1995), which strongly underestimate soil NO emissions at Bosco Fontana (see Section 2.4). This study suggests caution for using large-scale soil NO emission algorithms (including canopy reduction factors) for interpreting the soil NO contribution to biosphere-atmosphere NO_x exchange in polluted environments.

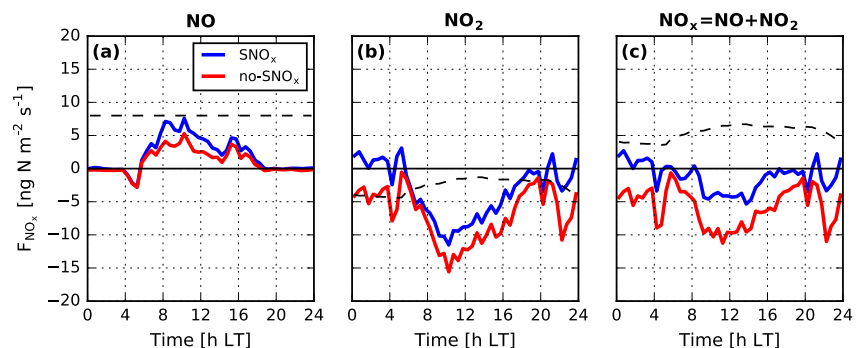


Figure 7. Canopy-top (26 m) fluxes of NO , NO_2 , and NO_x simulated by Multi-Layer Canopy-CHEMistry Exchange Model with (SNO_x) and without (no- SNO_x) soil NO_x exchange, and using the observation-derived vertical diffusivity in both simulations (Experiments 4 and 7 in Table 1). The black dashed lines indicate the soil fluxes for the SNO_x simulation.

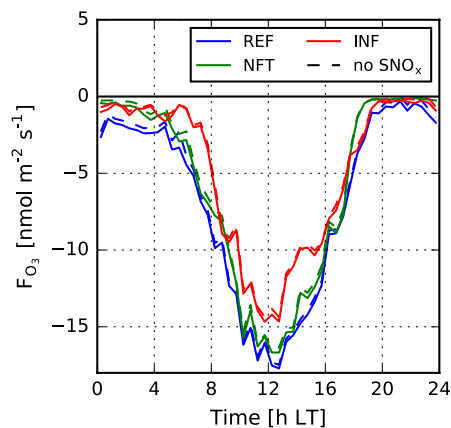


Figure 8. Campaign-median diurnal cycle of the total canopy ozone flux as simulated by Multi-Layer Canopy-Chemistry Exchange Model using reference vertical exchange (REF), vertical exchange derived using near-field theory, and observation-inferred vertical exchange. Solid lines indicate simulations with soil NO_x exchange, and dashed lines show simulations with deactivated soil NO_x exchange (i.e., soil NO emissions and soil NO_2 deposition).

3.5. Combined Impact of Vertical Mixing and Soil NO_x Exchange on Canopy Ozone Uptake

Next, we investigate the contribution by non-stomatal sinks, and particularly soil NO emissions, to canopy-scale ozone removal. We first derive the non-stomatal fraction of ozone deposition as the ratio between non-stomatal and total canopy conductance. On average during the campaign, this non-stomatal fraction is 65% in the INF simulation, our best estimate of canopy-atmosphere exchange and soil NO emissions. This fraction is 95% during nighttime (20–5 hr LT) due to in-active stomatal uptake, and substantially smaller during daytime (7–20 hr LT) at 38%.

In the INF simulation, lower-canopy chemical removal contributes $\pm 18\%$ to the total canopy ozone sink, depending on the representation of vertical exchange. Figure 8 displays the campaign-median diurnal cycle of the total ozone flux as simulated by MLC-CHEM, using the three different representations of vertical exchange, with and without considering soil NO_x exchange. However, the total ozone flux is only 5%–10% lower in simulations with deactivated soil NO_x exchange. Inside the canopy, chemical ozone removal competes with other ozone sinks. This suggests that the enhanced chemical ozone sink is compensated by reduced in-canopy ozone loss via deposition.

To further understand the weak sensitivity of the atmosphere-biosphere ozone flux to soil NO_x exchange, we analyze differences in simulated ozone formation and removal tendencies with and without soil NO_x exchange. The tendencies (unit: ppb h^{-1}) are calculated as the contribution of vertical exchange, deposition and chemical transformation to changes in ozone mixing ratios at each time step, following Ganzeveld, Lelieveld, Dentener, Krol, and Roelofs (2002). Campaign-average diurnal cycles of these tendencies are shown in Figure S4 in Supporting Information S1. The net upward soil NO_x exchange flux leads to changes in the diurnal variability in ozone tendencies, particularly in the lower canopy, but their diurnal variability remains similar. Therefore, we display diurnal averages of tendency changes due to soil NO_x exchange in Figure 9 for the three tested representations of vertical exchange, to explain the weak sensitivity of canopy-top ozone fluxes to soil NO_x exchange. Note that sinks result in negative ozone tendencies. As a result, an increased sink leads to a negative tendency change, while a decreased sink leads to a positive tendency change.

The chemical ozone sink is increased due to reaction with soil-emitted NO, reflected by a negative tendency change for ozone in the lower canopy (Figure 9). This introduces two compensating effects that both result in positive tendency changes: reduced deposition and increased vertical transport. Lower-canopy ozone deposition is reduced, because chemical removal and deposition are two competing sinks, acting on the ozone reservoir in the lower canopy. However, the reduced deposition sink does not fully compensate for the enhanced chemical ozone destruction. An additional compensating effect results from the dependence of vertical transport on the ozone gradient between the upper and lower canopy. The soil NO_x -induced chemical sink results in a larger vertical ozone gradient between the upper and lower canopy, and this increases vertical ozone transport into the lower canopy. These results do not strongly depend on the representation of vertical exchange (Figure 9). According to our analysis, reduced dry deposition and increased vertical transport together offset the enhanced lower-canopy ozone sink by reaction with soil NO.

4. Discussion

Our results show how vertical mixing conditions inside a forest differ from those in the atmospheric surface layer as a result of the presence of thermal inversions within the canopy. Accounting for these stability effects in the multi-layer canopy exchange model MLC-CHEM, by inferring the vertical diffusivity from observations (INF), leads to morning ozone deposition velocity decreases by up to 0.2–0.4 cm s^{-1} compared to two tested vertical exchange parameterizations in MLC-CHEM (REF and NFT), and in closer agreement with observations. In the afternoon, REF and NFT overestimate ozone deposition flux by on average 4.3 and 3.2 $\text{nmol m}^{-2} \text{s}^{-1}$, respectively, while INF agrees better with observations (MBE = 0.7 $\text{nmol m}^{-2} \text{s}^{-1}$). Given the dependence of in-canopy turbulence on stand density and vertical leaf area distribution (e.g., Banerjee & Linn, 2018; Russell et al., 2018),

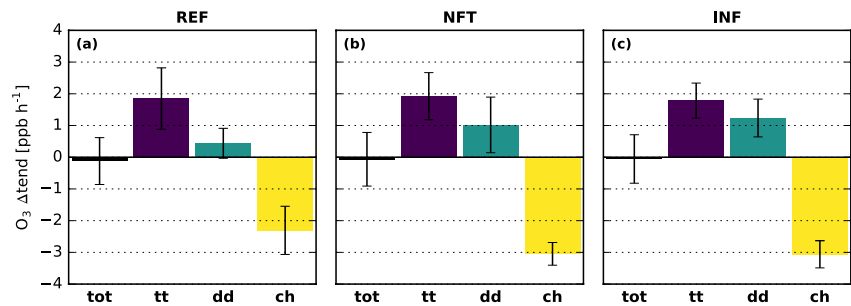


Figure 9. Change in lower-canopy ozone mean diurnal process tendencies as a result of soil NO_x exchange for three Multi-Layer Canopy-Chemistry Exchange Model simulation pairs using REF-, near-field theory-, and INF-based vertical exchange (a–c), respectively. Displayed tendency differences (tendency with soil NO_x exchange minus tendency without soil NO_x exchange) are due to changes turbulent transport (tt), dry deposition (dd), and chemistry (ch), as well as the resulting total tendency change (tot). Error bars indicate the standard deviation of the mean diurnal process tendencies.

this effect may be generalizable to closed forest canopies receiving high solar radiation. For these conditions, 3D atmospheric chemistry models, with highly parameterized vertical mixing inside and above forest canopies, could potentially overestimate atmosphere-biosphere exchange of ozone and other trace gases.

In our observation-based characterization of canopy-atmosphere exchange, we derived the vertical diffusivity from 30-min averages of temperature and the sensible heat flux. This is a common method to infer canopy-atmosphere exchange from observations (e.g., Brown et al., 2020) that incorporates effects of thermal stability on vertical exchange inside the canopy and between the canopy and the surface layer. This is an advancement compared to conventional methods to simulate in-canopy transport, used in deposition parameterizations applied in large-scale chemistry-transport models (e.g., Van Pul & Jacobs, 1994), which are based on above-canopy turbulence intensity (via the friction velocity) and canopy density (via LAI). However, the K-theory approach based on average fluxes and gradients does not account for non-local, intermittent sources of turbulence (Finnigan, 2000; Raupach, 1989). Previous work found variable effects of coherent structures to observed canopy-top fluxes: Thomas and Foken (2007) found a resulting 4% error in eddy-covariance fluxes, while Steiner et al. (2011) reported a 44%–65% contribution by coherent structures to the observed sensible heat flux.

The availability of ozone flux and mixing ratio observations along a vertical profile enables us to explore the similarity between K_H and a vertical diffusivity derived from 30-min averages of ozone flux and mixing ratio

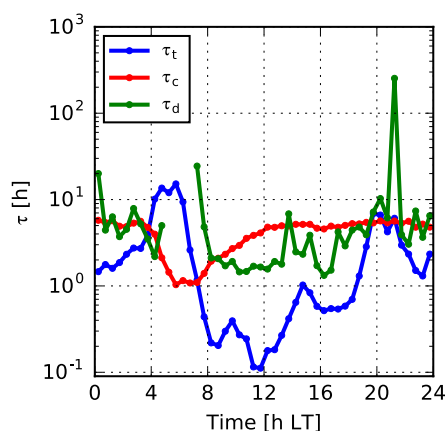


Figure 10. Campaign-averaged diurnal cycles of lifetimes against vertical transport (τ_t), chemical ozone loss by reaction with NO (τ_c) and deposition (τ_d) calculated from observations approximately at mid-canopy. Lifetimes are derived as follows: $\tau_t = \frac{1.1|h_c - z|^2}{K_H}$ (Gerken et al., 2017, with $z = 13$ m), $\tau_c = \frac{1}{k[\text{NO}]}$ (with $k = 1.9 \times 10^{14} \text{ s}^{-1}$ and $[\text{NO}]$ at 8 m), and $\tau_d = \frac{z}{v_d(\text{O}_3)}$ (with $z = 16$ m). Note that early morning τ_d values are omitted as they display erratic behavior due to near-zero ozone flux observations.

observations (K_{O_3}), shown in Figure S5 in Supporting Information S1. In the morning, K_{O_3} exceeds MLC-CHEM-simulated and observation-inferred K_H in the upper canopy (Figure S5a in Supporting Information S1). Finco et al. (2018) find an enhanced ozone flux at the canopy-atmosphere interface, possibly resulting from a local enhancement in NO mixing ratios at the canopy-top transported to this height from the soil and the surface layer. During the morning, with a relatively large vertical transport timescale ($\tau_t \approx 10$ hr, Figure 10) compared to the smaller timescale of chemical ozone loss by reaction with NO ($\tau_c \approx 1$ hr, Figure 10), we suspect that this enhanced flux will not change the ozone gradient between the canopy and the atmosphere, leading to an elevated K_{O_3} compared to K_H . During the afternoon, observation-derived values of K_H and K_{O_3} agree well, suggesting that chemical alteration of the ozone flux in the upper canopy dominantly occurs in the morning. Lower-canopy K_{O_3} exceeds K_H throughout the day (Figure S5b in Supporting Information S1), reflecting enhanced ozone removal due to the reaction between soil-emitted NO and ozone.

Our results highlight that canopy exchange of NO_x is driven by the vertical gradient in NO_x mixing ratios between the canopy and the surface layer. Soil NO emissions are high at our North-Italian study site, possibly due to high nitrogen deposition (de Vries et al., 2021) leading to nitrogen accumulation in the soil. We estimate that these soil emissions offset the total NO_x

deposition by 80%, and that soil-emitted NO is largely removed inside the forest. We conclude that information on canopy sources and sinks of NO_x, including soil NO emissions, is essential to understand the NO_x budget of forests, particularly in regions with high background levels of air pollution.

The campaign observations applied in this study indicate the presence of strong vertical gradients in NO_x and ozone mixing ratios in the lower canopy. Daytime NO_x mixing ratios measured directly above the soil are higher by up to 7 ppb compared to measurements at 5 m, while ozone mixing ratios above the soil (0.15 m) are ±20–55 ppb lower (Finco et al., 2018). These differences are caused by soil exchange processes (emissions of NO, deposition of NO₂ and ozone) and chemical reactions, amplified by the very stable stratification at this height. This near-surface effect is important for evaluating the contribution of soil emissions to the canopy NO_x exchange budget, as our results show that the soil NO_x flux inferred from above-soil enclosure chamber measurements cannot be reconciled with the observed NO_x mixing ratios at 6.5 m (Figure S3 in Supporting Information S1), likely indicating NO_x loss near the forest floor. Resolving these gradients requires an increased vertical resolution in MLC-CHEM. Our choice for a model with two canopy layers is justified by the applicability of this model version in regional/global models (Ganzeveld, Lelieveld, Dentener, Krol, & Roelofs, 2002; Ganzeveld et al., 2010), and the availability of observational constraints at two heights in the canopy. The strong vertical gradients in ozone mixing ratios are unlikely to be caused by VOC-ozone reactions, since the contribution of measured VOCs to the total ozone flux at Bosco Fontana is very small (Finco et al., 2018). However, we cannot rule out that unmeasured, highly reactive compounds could have contributed to in-canopy ozone removal (Goldstein et al., 2004; Vermeuel et al., 2021).

To further investigate potential sub-grid vertical gradients, we derive mid-canopy lifetimes against vertical transport, chemical loss and deposition (Figure 10). If the lifetime against vertical transport (τ_v) is of a similar magnitude as the lifetime of other processes, replenishment is not sufficiently fast to counter chemical loss or deposition, leading to sharp vertical ozone gradients that are challenging to resolve in multi-layer canopy models. During the early morning and evening, τ_v is indeed of a similar or higher magnitude compared to τ_c and τ_d . During daytime, however, vertical ozone transport is much faster than chemical loss and deposition, indicating that the mid-canopy is well-mixed. However, sharp ozone and NO_x gradients occur directly above the soil (Finco et al., 2018), which occurs at the subgrid-scale in MLC-CHEM.

The aforementioned shortcomings could be addressed by application of a Large-Eddy Simulation (LES) model coupled to a multi-layer canopy model to study ozone deposition (hereafter LES-MLC). Recently, LES simulations of canopy turbulence have been performed under varying atmospheric stability (e.g., Patton et al., 2016), and Clifton and Patton (2021) have extended this approach with ozone uptake. These models advantageously resolve turbulent motions at a larger range of length scales, and have an in-canopy vertical resolution on the order of several meters. Therefore, LES models are an appropriate tool to investigate vertical gradients in turbulent exchange inside and directly above forest canopies, and how this affects canopy-atmosphere exchange of NO_x and ozone. As a future line of research, we propose to apply coupled LES-MLC models to improve mechanistic understanding of the interaction between in-canopy turbulent mixing gradients and ozone removal processes. For example, LES-MLC models can be applied to investigate how vegetated canopies affect chemical ozone flux divergence (Vila-Guerau De Arellano et al., 1993), and to test how this affects the (dis)similarity between vertical diffusivities for sensible heat and trace gases (Figure S5 in Supporting Information S1). This would require performing LES-MLC simulations that closely mimic site conditions at selected observational sites with detailed observations of in-canopy turbulence and trace gas exchange fluxes, which is an area of ongoing research (Bannister et al., 2022). The proposed developments have large potential to improve the representation of turbulent exchange in multi-layer canopy exchange models (e.g., MLC-CHEM) that can be applied in coupled 3D atmospheric chemistry model experiments used for air quality assessments and chemistry-climate studies.

5. Conclusions

We quantified the impact of forest-atmosphere turbulent exchange and soil NO_x exchange on ozone deposition in a polluted Italian forest. We applied a multi-layer canopy exchange model (MLC-CHEM) to interpret campaign observations of NO_x and ozone mixing ratios and ozone fluxes. Vertical mixing conditions in the dense Bosco Fontana forest canopy are fully or partially decoupled from the surface layer during large parts of the campaign, posing challenges for simulating ozone deposition. Two common parameterizations of canopy-atmosphere

exchange overestimate the observation-derived in-canopy vertical mixing. Accounting for observed vertical exchange in our simulations decreases the simulated deposition velocity by up to 0.2–0.4 cm s⁻¹ (>100%) when canopy-atmosphere exchange is weak, and in closer agreement with observations.

The soil contributes substantially to NO_x levels in the lower canopy (45% on average), which is remarkable given the observed high background NO_x mixing ratios (4 ppb during daytime). Soil NO-ozone chemistry accounts for 18% of the total canopy ozone sink. However, the magnitude of the canopy-top ozone deposition flux is hardly affected by the soil NO-ozone reaction. This is partly because the enhanced chemical ozone sink leads to reduced dry deposition to the soil and understory vegetation, and partly due to enhanced downward ozone transport as the lower canopy becomes a stronger sink.

Our results highlight how the complex nature of vertical mixing in forests affects canopy-atmosphere exchange of reactive trace gases. We suggest to apply turbulence-resolving models coupled to multi-layer canopy models of trace gas exchange to interpret field observations. This approach advances our understanding of the interaction between in-canopy turbulence and ozone sinks, and can lead to improved canopy-atmosphere exchange parameterizations in larger-scale atmospheric chemistry models. This enables a better quantification of the land surface ozone sink and its impacts on surface ozone mixing ratios and ecosystem carbon uptake.

Data Availability Statement

Data used in the creation of Figure 1 can be obtained from the following in-text references (Beguería, 2017; Holmes & Ducker, 2018). Observational data from the ECLAIRE field campaign are freely available upon registration on the ECLAIRE Data Portal (<https://eclairadata.ceh.ac.uk/page/login.aspx>). Registration is required following the data sharing protocol of the ECLAIRE project. The MLC-CHEM model version and model output used in this study are stored at the 4TU.ResearchData repository (<https://doi.org/10.4121/19727287>).

Acknowledgments

AJV thanks Jordi Vilà-Guerau de Arellano for the discussions that led to the conception of this study. AVJ was supported by the Dutch Research Council (Grant ALW-GO 16/17). MCK received funding from the European Research Council (ERC) under the European Union's Horizon 2020 Research and Innovation Programme (Grant agreement 742798). The Bosco Fontana measurement campaign was funded by the European Commission Seventh Framework Programme (collaborative projects "ECLAIRE," Grant 282910). The authors thank two anonymous reviewers for the constructive feedback that helped improve this work.

References

- Agyei, T., Juráň, S., Kwakye, K. O. A., Šigut, L., Urban, O., & Marek, M. V. (2020). The impact of drought on total ozone flux in a mountain Norway spruce forest. *Journal of Forest Science*, 66(7), 280–287. <https://doi.org/10.17221/129/2019-JFS>
- Ainsworth, E., Yendrek, C. R., Sitch, S., Collins, W. J., & Emberson, L. D. (2012). The effects of tropospheric ozone on net primary productivity and implications for climate change. *Annual Review of Plant Biology*, 63(1), 637–661. <https://doi.org/10.1146/annurev-arplant-042110-103829>
- Ashworth, K., Chung, S. H., Griffin, R. J., Chen, J., Forkel, R., Bryan, A. M., & Steiner, A. L. (2015). FORest Canopy Atmosphere Transfer (FORCAST) 1.0: A 1-D model of biosphere-atmosphere chemical exchange. *Geoscientific Model Development*, 8(11), 3765–3784. <https://doi.org/10.5194/gmd-8-3765-2015>
- Banerjee, T., & Linn, R. (2018). Effect of vertical canopy architecture on transpiration, thermoregulation and carbon assimilation. *Forests*, 9(4), 198. <https://doi.org/10.3390/f9040198>
- Bannister, E. J., MacKenzie, A. R., & Cai, X. (2022). Realistic forests and the modeling of forest-atmosphere exchange. *Reviews of Geophysics*, 60(1), 1–47. <https://doi.org/10.1029/2021rg000746>
- Bates, K. H., & Jacob, D. J. (2020). An expanded definition of the odd oxygen family for tropospheric ozone budgets: Implications for ozone lifetime and stratospheric influence. *Geophysical Research Letters*, 47(4), 1–9. <https://doi.org/10.1029/2019GL084486>
- Beguería, S. (2017). SPEIbase: Version 2.5.1 [Dataset]. Zenodo. <https://doi.org/10.5281/zenodo.834462>
- Brown, J. S., Shapkalijevski, M. M., Krol, M. C., Karl, T., Ouwensloot, H. G., Moene, A. F., et al. (2020). Ozone exchange within and above an irrigated Californian orchard. *Tellus Series B Chemical and Physical Meteorology*, 72(1), 1–17. <https://doi.org/10.1080/16000889.2020.1723346>
- Cionco, R. M. (1978). Analysis of canopy index values for various canopy densities. *Boundary-Layer Meteorology*, 15(1), 81–93. <https://doi.org/10.1007/BF00165507>
- Clifton, O. E., Fiore, A. M., Massman, W. J., Baublitz, C. B., Coyle, M., Emberson, L., et al. (2020). Dry deposition of ozone over land: Processes, measurement, and modeling. *Reviews of Geophysics*, 58(1), e2019RG000670. <https://doi.org/10.1029/2019RG000670>
- Clifton, O. E., Fiore, A. M., Munger, J. W., Malyshev, S., Horowitz, L. W., Shevliakova, E., et al. (2017). Interannual variability in ozone removal by a temperate deciduous forest. *Geophysical Research Letters*, 44(1), 542–552. <https://doi.org/10.1002/2016GL070923>
- Clifton, O. E., & Patton, E. G. (2021). Does organization in turbulence influence ozone removal by deciduous forests? *Journal of Geophysical Research: Biogeosciences*, 126(6), 1–20. <https://doi.org/10.1029/2021JG006362>
- de Vries, W., Schulte-Uebbing, L., Kros, H., Voogd, J. C., & Louwagie, G. (2021). Spatially explicit boundaries for agricultural nitrogen inputs in the European Union to meet air and water quality targets. *Science of the Total Environment*, 786, 147283. <https://doi.org/10.1016/j.scitotenv.2021.147283>
- Delaria, E. R., Vieira, M., Cremieux, J., & Cohen, R. C. (2018). Measurements of NO and NO₂ exchange between the atmosphere and *Quercus agrifolia*. *Atmospheric Chemistry and Physics*, 18(19), 14161–14173. <https://doi.org/10.5194/acp-18-14161-2018>
- Dorsey, J. R., Duyzer, J. H., Gallagher, M. W., Coe, H., Pilegaard, K., Weststrate, J. H., et al. (2004). Oxidized nitrogen and ozone interaction with forests. I: Experimental observations and analysis of exchange with Douglas fir. *Quarterly Journal of the Royal Meteorological Society*, 130(600), 1941–1955. <https://doi.org/10.1256/qj.03.124>
- Ducker, J. A., Holmes, C. D., Keenan, T. F., Fares, S., Goldstein, A. H., Mammarella, I., et al. (2018). Synthetic ozone deposition and stomatal uptake at flux tower sites. *Biogeosciences*, 15(17), 5395–5413. <https://doi.org/10.5194/bg-15-5395-2018>

- Duyzer, J. H., Dorsey, J. R., Gallagher, M. W., Pilegaard, K., & Walton, S. (2004). Oxidized nitrogen and ozone interaction with forests. II: Multi-layer process-oriented modelling results and a sensitivity study for Douglas fir. *Quarterly Journal of the Royal Meteorological Society*, *130*(600), 1957–1971. <https://doi.org/10.1256/qj.03.125>
- El-Madany, T. S., Niklasch, K., & Klemm, O. (2017). Stomatal and non-stomatal turbulent deposition flux of ozone to a managed peatland. *Atmosphere*, *8*(9), 1–16. <https://doi.org/10.3390/atmos8090175>
- Fares, S., Savi, F., Muller, J., Matteucci, G., & Paoletti, E. (2014). Simultaneous measurements of above and below canopy ozone fluxes help partitioning ozone deposition between its various sinks in a Mediterranean Oak Forest. *Agricultural and Forest Meteorology*, *198*, 181–191. <https://doi.org/10.1016/j.agrformet.2014.08.014>
- Fares, S., Weber, R., Park, J. H., Gentner, D., Karlik, J., & Goldstein, A. H. (2012). Ozone deposition to an orange orchard: Partitioning between stomatal and non-stomatal sinks. *Environmental Pollution*, *169*, 258–266. <https://doi.org/10.1016/j.envpol.2012.01.030>
- Finco, A., Coyle, M., Nemitz, E., Marzuoli, R., Chiesa, M., Loubet, B., et al. (2018). Characterization of ozone deposition to a mixed oak-hornbeam forest-flux measurements at five levels above and inside the canopy and their interactions with nitric oxide. *Atmospheric Chemistry and Physics*, *18*(24), 17945–17961. <https://doi.org/10.5194/acp-18-17945-2018>
- Finnigan, J. J. (2000). Turbulence in plant canopies. *Annual Review of Fluid Mechanics*, *32*(1), 519–571. <https://doi.org/10.1146/annurev.fluid.32.1.519>
- Foken, T., Meixner, F. X., Falge, E., Zetzsch, C., Serafimovich, A., Bargsten, A., et al. (2012). Coupling processes and exchange of energy and reactive and non-reactive trace gases at a forest site—results of the EGER experiment. *Atmospheric Chemistry and Physics*, *12*(4), 1923–1950. <https://doi.org/10.5194/acp-12-1923-2012>
- Fowler, D., Pilegaard, K., Sutton, M. A., Ambus, P., Raivonen, M., Duyzer, J., et al. (2009). Atmospheric composition change: Ecosystems-Atmosphere interactions. *Atmospheric Environment*, *43*(33), 5193–5267. <https://doi.org/10.1016/j.atmosenv.2009.07.068>
- Galmardini, S., Makar, P., Clifton, O. E., Hogrefe, C., Bash, J., Bellasio, R., et al. (2021). AQMEII4 activity 1: Evaluation of wet and dry deposition schemes as an integral part of regional-scale air quality models. *Atmospheric Chemistry and Physics Discussions*, *21*(20), 15663–15697. <https://doi.org/10.5194/acp-2021-313>
- Ganzeveld, L. N., Bouwman, L., Stehfest, E., van Vuuren, D., Eickhout, B., & Lelieveld, J. (2010). Impacts of future land cover changes on atmospheric chemistry-climate interactions. *Journal of Geophysical Research*, *115*, D23301. <https://doi.org/10.1029/2010JD014041>
- Ganzeveld, L. N., & Lelieveld, J. (1995). Dry deposition parameterization in a chemistry general circulation model and its influence on the distribution of reactive trace gases. *Journal of Geophysical Research*, *100*(D10), 20999–21012. <https://doi.org/10.1029/95jd02266>
- Ganzeveld, L. N., Lelieveld, J., Dentener, F. J., Krol, M. C., Bouwman, A. J., & Roelofs, G. J. (2002). Global soil-biogenic NO_x emissions and the role of canopy processes. *Journal of Geophysical Research*, *107*(16), 1–17. <https://doi.org/10.1029/2001JD001289>
- Ganzeveld, L. N., Lelieveld, J., Dentener, F. J., Krol, M. C., & Roelofs, G. J. (2002). Atmosphere-biosphere trace gas exchanges simulated with a single-column model. *Journal of Geophysical Research*, *107*(16), 1–21. <https://doi.org/10.1029/2001JD000684>
- Ganzeveld, L. N., Lelieveld, J., & Roelofs, G. J. (1998). A dry deposition parameterization for sulfur oxides in a chemistry and general circulation model. *Journal of Geophysical Research*, *103*(D5), 5679–5694. <https://doi.org/10.1029/97JD03077>
- Gerken, T., Chamecki, M., & Fuentes, J. D. (2017). Air-parcel residence times within forest canopies. *Boundary-Layer Meteorology*, *165*(1), 29–54. <https://doi.org/10.1007/s10546-017-0269-7>
- Gerosa, G., Marzuoli, R., Monteleone, B., Chiesa, M., & Finco, A. (2017). Vertical ozone gradients above forests. Comparison of different calculation options with direct ozone measurements above a mature forest and consequences for ozone risk assessment. *Forests*, *8*(9), 337. <https://doi.org/10.3390/f8090337>
- Goldstein, A. H., McKay, M., Kurpius, M. R., Schade, G. W., Lee, A., Holzinger, R., & Rasmussen, R. A. (2004). Forest thinning experiment confirms ozone deposition to forest canopy is dominated by reaction with biogenic VOCs. *Geophysical Research Letters*, *31*(22), 1–4. <https://doi.org/10.1029/2004GL021259>
- Guenther, A. B., Jiang, X., Heald, C. L., Sakulyanontvittaya, T., Duhl, T., Emmons, L. K., & Wang, X. (2012). The model of emissions of gases and aerosols from nature version 2.1 (MEGAN2.1): An extended and updated framework for modeling biogenic emissions. *Geoscientific Model Development*, *5*(6), 1471–1492. <https://doi.org/10.5194/gmd-5-1471-2012>
- Hardacre, C., Wild, O., & Emberson, L. (2015). An evaluation of ozone dry deposition in global scale chemistry climate models. *Atmospheric Chemistry and Physics*, *15*(11), 6419–6436. <https://doi.org/10.5194/acpd-14-22793-2014>
- Holmes, C. D., & Ducker, J. A. (2018). SynFlux: A synthetic dataset of atmospheric deposition and stomatal uptake at flux tower sites (1.1) [Dataset]. Zenodo. <https://doi.org/10.5281/zenodo.1402054>
- Hu, L., Jacob, D. J., Liu, X., Zhang, Y., Zhang, L., Kim, P. S., et al. (2017). Global budget of tropospheric ozone: Evaluating recent model advances with satellite (OMI), aircraft (IAGOS), and ozonesonde observations. *Atmospheric Environment*, *167*, 323–334. <https://doi.org/10.1016/j.atmosenv.2017.08.036>
- Jocher, G., Marshall, J., Nilsson, M. B., Linder, S., De Simon, G., Hörnlund, T., et al. (2018). Impact of canopy decoupling and subcanopy advection on the annual carbon balance of a boreal scots pine forest as derived from eddy covariance. *Journal of Geophysical Research: Biogeosciences*, *123*(2), 303–325. <https://doi.org/10.1002/2017JG003988>
- Kuenen, J., Dellaert, S., Visschedijk, A., Jalkanen, J. P., Super, I., & Denier Van Der Gon, H. (2022). CAMS-REG-v4: A state-of-the-art high-resolution European emission inventory for air quality modelling. *Earth System Science Data*, *14*(2), 491–515. <https://doi.org/10.5194/essd-14-491-2022>
- Lin, M., Horowitz, L. W., Xie, Y., Paulot, F., Malyshev, S., Shevliakova, E., et al. (2020). Vegetation feedbacks during drought exacerbate ozone air pollution extremes in Europe. *Nature Climate Change*, *10*(5), 444–451. <https://doi.org/10.1038/s41558-020-0743-y>
- Makar, P. A., Staebler, R. M., Akingunola, A., Zhang, J., McLinden, C., Kharol, S. K., et al. (2017). The effects of forest canopy shading and turbulence on boundary layer ozone. *Nature Communications*, *8*(1), 1–14. <https://doi.org/10.1038/ncomms15243>
- Mölder, M., Grelle, A., Lindroth, A., & Halldin, S. (1999). Flux-profile relationships over a boreal forest—roughness sublayer corrections. *Agricultural and Forest Meteorology*, *98–99*, 645–658. [https://doi.org/10.1016/S0168-1923\(99\)00131-8](https://doi.org/10.1016/S0168-1923(99)00131-8)
- Monteith, J. (1965). Evaporation and environment. *Symposia of the Society for Experimental Biology*, *19*, 205–234. Retrieved from <https://repository.rothamsted.ac.uk/item/8v5v7>
- Neirynek, J., Gielen, B., Janssens, I. A., & Ceulemans, R. (2012). Insights into ozone deposition patterns from decade-long ozone flux measurements over a mixed temperate forest. *Journal of Environmental Monitoring*, *14*(6), 1684–1695. <https://doi.org/10.1039/c2em10937a>
- Otu-Larbi, F., Conte, A., Fares, S., Wild, O., & Ashworth, K. (2021). FORCAsT-gs: Importance of stomatal conductance parameterization to estimated ozone deposition velocity. *Journal of Advances in Modeling Earth Systems*, *13*(9), 1–23. <https://doi.org/10.1029/2021ms002581>
- Patton, E. G., Sullivan, P. P., Shaw, R. H., Finnigan, J. J., & Weil, J. C. (2016). Atmospheric stability influences on coupled boundary layer and canopy turbulence. *Journal of the Atmospheric Sciences*, *73*(4), 1621–1647. <https://doi.org/10.1175/JAS-D-15-0068.1>

- Pilegaard, K., Skiba, U., Ambus, P., Beier, C., Brüggemann, N., Butterbach-Bahl, K., et al. (2006). Factors controlling regional differences in forest soil emission of nitrogen oxides (NO and N₂O). *Biogeosciences*, 3(4), 651–661. <https://doi.org/10.5194/bg-3-651-2006>
- Raivonen, M., Vesala, T., Pirjola, L., Altimir, N., Keronen, P., Kulmala, M., & Hari, P. (2009). Compensation point of NO_x exchange: Net result of NO_x consumption and production. *Agricultural and Forest Meteorology*, 149(6–7), 1073–1081. <https://doi.org/10.1016/j.agrformet.2009.01.003>
- Rannik, Ü., Altimir, N., Mammarella, I., Bäck, J., Rinne, J., Ruuskanen, T. M., et al. (2012). Ozone deposition into a boreal forest over a decade of observations: Evaluating deposition partitioning and driving variables. *Atmospheric Chemistry and Physics*, 12(24), 12165–12182. <https://doi.org/10.5194/acp-12-12165-2012>
- Raupach, M. R. (1989). A practical Lagrangian method for relating scalar concentrations to source distributions in vegetation canopies. *Quarterly Journal of the Royal Meteorological Society*, 115(487), 609–632. <https://doi.org/10.1002/qj.49711548710>
- Ronda, R., De Bruin, H., & Holtslag, A. (2001). Representation of the canopy conductance in modeling the surface energy budget for low vegetation. *Journal of Applied Meteorology*, 40(8), 1431–1444. [https://doi.org/10.1175/1520-0450\(2001\)040<1431:ROTCCI>2.0.CO;2](https://doi.org/10.1175/1520-0450(2001)040<1431:ROTCCI>2.0.CO;2)
- Rummel, U., Ammann, C., Kirkman, G. A., Moura, M. A., Foken, T., Andreae, M. O., & Meixner, F. X. (2007). Seasonal variation of ozone deposition to a tropical rain forest in southwest Amazonia. *Atmospheric Chemistry and Physics*, 7(20), 5415–5435. <https://doi.org/10.5194/acp-7-5415-2007>
- Russell, E. S., Liu, H., Thistle, H., Strom, B., Greer, M., & Lamb, B. (2018). Effects of thinning a forest stand on sub-canopy turbulence. *Agricultural and Forest Meteorology*, 248, 295–305. <https://doi.org/10.1016/j.agrformet.2017.10.019>
- Skiba, U., Medinets, S., Cardenas, L. M., Carnell, E. J., Hutchings, N. J., & Amon, B. (2021). Assessing the contribution of soil NO_x emissions to European atmospheric pollution. *Environmental Research Letters*, 16(2), 025009. <https://doi.org/10.1088/1748-9326/abd2f2>
- Steiner, A. L., Pressley, S. N., Botros, A., Jones, E., Chung, S. H., & Edburg, S. L. (2011). Analysis of coherent structures and atmosphere-canopy coupling strength during the CABINEX field campaign. *Atmospheric Chemistry and Physics*, 11(23), 11921–11936. <https://doi.org/10.5194/acp-11-11921-2011>
- Teklemariam, T. A., & Sparks, J. P. (2006). Leaf fluxes of NO and NO₂ in four herbaceous plant species: The role of ascorbic acid. *Atmospheric Environment*, 40(12), 2235–2244. <https://doi.org/10.1016/j.atmosenv.2005.12.010>
- Thomas, C., & Foken, T. (2007). Flux contribution of coherent structures and its implications for the exchange of energy and matter in a tall spruce canopy. *Boundary-Layer Meteorology*, 123(2), 317–337. <https://doi.org/10.1007/s10546-006-9144-7>
- Van Pul, W., & Jacobs, A. (1994). The conductance of a maize crop and the underlying soil to ozone under various environmental conditions. *Boundary-Layer Meteorology*, 69(1–2), 83–99. <https://doi.org/10.1007/bf00713296>
- Vermeuel, M. P., Cleary, P. A., Desai, A. R., & Bertram, T. H. (2021). Simultaneous measurements of O₃ and HCOOH vertical fluxes indicate rapid in-canopy terpene chemistry enhances O₃ removal over mixed temperate forests. *Geophysical Research Letters*, 48(3), 1–15. <https://doi.org/10.1029/2020GL090996>
- Vila-Guerau De Arellano, J., Duynkerke, P. G., & Bultjes, P. J. (1993). The divergence of the turbulent diffusion flux in the surface layer due to chemical reactions: The NO-O₃-NO₂ system. *Tellus B: Chemical and Physical Meteorology*, 45(1), 23–33. <https://doi.org/10.3402/tellusb.v45i1.15576>
- Vinken, G. C. M., Boersma, K. F., Maasakkers, J. D., Adon, M., & Martin, R. V. (2014). Worldwide biogenic soil NO_x emissions inferred from OMI NO₂ observations. *Atmospheric Chemistry and Physics*, 14(18), 10363–10381. <https://doi.org/10.5194/acp-14-10363-2014>
- Visser, A. J., Boersma, K. F., Ganzeveld, L. N., & Krol, M. C. (2019). European NO_x emissions in WRF-Chem derived from OMI: Impacts on summertime surface ozone. *Atmospheric Chemistry and Physics*, 19(18), 11821–11841. <https://doi.org/10.5194/acp-2019-295>
- Visser, A. J., Ganzeveld, L. N., Godeed, I., Krol, M. C., Mammarella, I., Manca, G., & Boersma, K. F. (2021). Ozone deposition impact assessments for forest canopies require accurate ozone flux partitioning on diurnal timescales. *Atmospheric Chemistry and Physics*, 21(24), 18393–18411. <https://doi.org/10.5194/acp-21-18393-2021>
- Wang, W., Ganzeveld, L., Rossabi, S., Hueber, J., & Helmig, D. (2020). Measurement report: Leaf-scale gas exchange of atmospheric reactive trace species (NO₂, NO, O₃) at a northern hardwood forest in Michigan. *Atmospheric Chemistry and Physics*, 20(19), 11287–11304. <https://doi.org/10.5194/acp-20-11287-2020>
- Willmott, C. (1982). Some comments on the evaluation of model performance. *Bulletin of the American Meteorological Society*, 63(11), 1309–1313. [https://doi.org/10.1175/1520-0477\(1982\)063<1309:SCOTEO>2.0.CO;2](https://doi.org/10.1175/1520-0477(1982)063<1309:SCOTEO>2.0.CO;2)
- Wong, A. Y., Geddes, J. A., Ducker, J. A., Holmes, C. D., Fares, S., Goldstein, A. H., et al. (2022). New evidence for the importance of non-stomatal pathways in ozone deposition during extreme heat and dry anomalies. *Geophysical Research Letters*, 49(8), 1–12. <https://doi.org/10.1029/2021GL095717>
- Wu, Z., Schwede, D. B., Vet, R., Walker, J. T., Shaw, M., Staebler, R., & Zhang, L. (2018). Evaluation and intercomparison of five North American dry deposition algorithms at a mixed forest site. *Journal of Advances in Modeling Earth Systems*, 10(7), 1571–1586. <https://doi.org/10.1029/2017MS001231>
- Yienger, J., & Levy, H. (1995). Empirical model of global soil-biogenic NO_x emissions. *Journal of Geophysical Research*, 100(D6), 447–458. <https://doi.org/10.1029/95JD00370>
- Young, P. J., Naik, V., Fiore, A. M., Gaudel, A., Guo, J., Lin, M. Y., et al. (2018). Tropospheric Ozone Assessment Report: Assessment of global-scale model performance for global and regional ozone distributions, variability, and trends. *Elementa: Science of the Anthropocene*, 6, 10. <https://doi.org/10.1525/elementa.265>

References From the Supporting Information

- Vicente-Serrano, S. M., Beguería, S., & López-Moreno, J. I. (2010). A multiscalar drought index sensitive to global warming: The standardized precipitation evapotranspiration index. *Journal of Climate*, 23(7), 1696–1718. <https://doi.org/10.1175/2009JCL12909.1>